(NASA-CR-151514) [illegible] N77-24[illegible]
[illegible] Interim Report, [illegible]
[illegible] (Virginia Polytechnic [illegible]

COLLEGE OF ENGINEERING

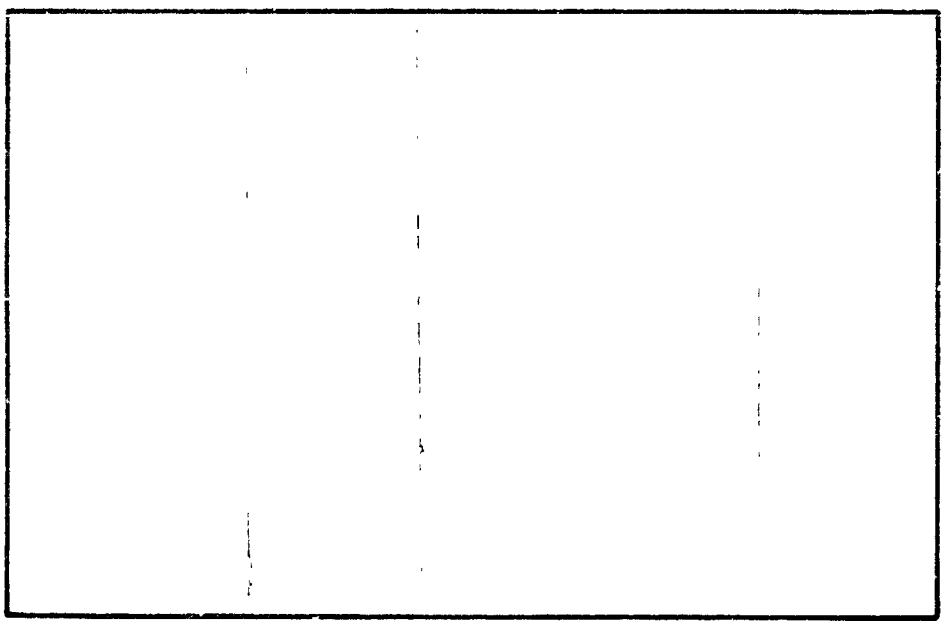

VIRGINIA POLYTECHNIC INSTITUTE AND STATE UNIVERSITY

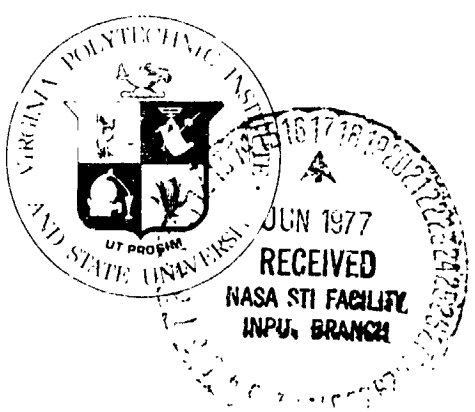

JUN 1977
RECEIVED
NASA STI FACILITY
INPUT BRANCH

BLACKSBURG, VIRGINIA

College of Engineering
Virginia Polytechnic Institute and State University
Blacksburg, VA 24061

VPI-E-77-15 May 1977

A STUDY OF DAMAGE ZONES OR CHARACTERISTIC LENGTHS AS RELATED TO THE FRACTURE BEHAVIOR OF GRAPHITE/EPOXY LAMINATES

Y. T. Yeow, Research Associate
H. F. Brinson, Professor

Department of Engineering Science and Mechanics

Prepared for:

National Aeronautics and Space Administration
Grant No. NASA-NSG 2038
Materials Science Branch
Ames Research Center
Moffett Field, CA 94035

Approved for Public Release; distribution unlimited.

BIBLIOGRAPHIC DATA SHEET	1. Report No. VPI-E-77-15	2.	3. Recipient's Accession No.
4. Title and Subtitle A STUDY OF DAMAGE ZONES OR CHARACTERISTIC LENGTHS AS RELATED TO THE FRACTURE BEHAVIOR OF GRAPHITE/EPOXY LAMINATES			5. Report Date May 1977 6.
7. Author(s) Y. T. Yeow, H. F. Brinson			8. Performing Organization Rept. No. VPI-E-77-15
9. Performing Organization Name and Address Engineering Science and Mechanics Virginia Polytechnic Inst. & State University Blacksburg, VA 24061			10. Project/Task/Work Unit No. 11. Contract/Grant No. NASA-NSG-2038
12. Sponsoring Organization Name and Address NASA Materials Science Branch Ames Research Center Moffett Field, CA 94035			13. Type of Report & Period Covered Interim 10/1/76-9/30/77 14.
15. Supplementary Notes			

16. Abstracts
The results of uniaxial tensile tests conducted on a variety of graphite/epoxy laminates containing narrow rectangular slits, square or circular holes with various aspect ratios are discussed. The techniques used to study stable crack or damage zone growth--namely, birefringence coatings, COD gages, and microscopic observations are discussed. Initial and final fracture modes are discussed as well as the effect of notch size and shape and laminate type on the fracture process. Characteristic lengths are calculated and compared to each other using the point, average and inherent flaw theories. Fracture toughnesses are calculated by the same theories and compared to a boundary integral equation technique. Finite width K-calibration factors are also discussed.

17. Key Words and Document Analysis. 17a. Descriptors
fracture, damage zones, characteristic lengths, graphite/epoxy laminates

17b. Identifiers/Open-Ended Terms

17c. COSATI Field/Group

18. Availability Statement	19. Security Class (This Report)	21. No. of Pages
Distribution unlimited	UNCLASSIFIED	
	20. Security Class (This Page) UNCLASSIFIED	22. Price

FORM NTIS-35 (REV 10-73) ENDORSED BY ANSI AND UNESCO. THIS FORM MAY BE REPRODUCED USCOMM-DC 82-S-P74

Abstract

The results of uniaxial tensile tests conducted on a variety of graphite/epoxy laminates containing narrow rectangular slits, square or circular holes with various aspect ratios are discussed. The techniques used to study stable crack or damage zone growth--namely, birefringence coatings, COD gages, and microscopic observations are discussed. Initial and final fracture modes are discussed as well as the effect of notch size and shape and laminate type on the fracture process. Characteristic lengths are calculated and compared to each other using the point, average and inherent flaw theories. Fracture toughnesses are calculated by the same theories and compared to a boundary integral equation technique. Finite width K-calibration factors are also discussed.

Introduction

Many efforts have been made to use linear elastic fracture mechanics (LEFM) to interpret the fracture behavior of fiber reinforced materials [1-11]. In general, these investigations have shown usual LEFM techniques to be an adequate analytical tool only under a limited set of circumstances. A common practice by a number of investigators has been the incorporation of a damage zone or characteristic length ahead of the implanted flaw. With this procedure, fracture has been defined to occur when the size of the damage zone reached a critical value analogous to the method of incorporating yielding into LEFM for metals. To date, the damage zone size or characteristic length has been shown to be a material and geometrical property as studies have shown the dimension to be both dependent upon the length of flaw and type of composite material.

Obviously, the measurement or quantification of the damage zone size is of paramount importance if LEFM which includes the parameter are to be used in the design of composite structures. Among the methods presently in use for this purpose are photoelastic coatings,[12] idealized photoelastic models,[13] scanning electron microscopy,[14,15] thermography,[16] special x-ray procedures[17] and crack opening displacement (COD) gages.[8] In this connection, perhaps the least defined and the most controversial issue is the question of what constitutes failure and damage.

The purpose of the study contained herein was to investigate the nature and cause of the intense energy or stress field in front of notches or cracks as tensile samples were ramp loaded to failure. The experimental techniques selected for use were the COD gage, in-situ microscopic

observations, photoelastic coatings and post-mortem microscopic examinations. Laminate orientations of $[0°]_{8s}$, $[0°/90°]_{4s}$, $[0°/\pm45°/0°]_{2s}$ and $[\pm45°]_{4s}$ of T300/934 graphite/epoxy materials were investigated. These orientations were selected to provide a range of properties from quasi-isotropic to orthotropic and highly anisotropic. The notch geometries selected for three laminate orientations were crack-like slits and square cutouts or slots. Four aspect ratios were studied for the purpose of measuring notch sensitivity effects as a function of both cutout width and height. That is, comparison of notch effects for square slots to those of crack-like slits was to be performed for each aspect ratio. The $[\pm45°]$ laminates were investigated using slits and holes of the same aspect ratio for the purpose of comparing notch effects for these two geometries for this one laminate.

Experimental Procedures

The 16 ply panels of T300/934 graphite/epoxy were manufactured by Lockheed, Sunnyvale. Tensile strip specimens with dimensions of 1 in x 10 in x 0.1 in (2.54 cm x 25.4 cm x 0.254 cm) were cut from the panels using a diamond impregnated wheel or saw. Fiberglass end tabs were bonded to the specimens such that the unreinforced length was approximately 7 in (15.24 cm). Crack-like slits and square slots were ultrasonically machined in the center of the $[0°]_{8s}$, $[0°/\pm45°/0°]_{2s}$ and $[0°/90°]_{4s}$ laminate samples. Similarly, slits and holes were machined in the center of the $[\pm45°]_{4s}$ laminate samples. The slit height (dimension parallel to the load) was approximately 0.01 in (0.0254 cm) in all cases. The aspect ratios (slit width to specimen width, 2a/w) varied

from 0.15 to 0.45 with increments of 0.1 for all geometries, i.e., narrow slits, square slots, and circular holes.

Three replicates of each notch geometry were tested in tension using an MTS closed loop hydraulic testing machine at a head-rate of 0.05 in/min (0.127 cm/min).* Two replicates each contained a photoelastic coating. In-situ microscopic observations and COD measurements were made on the third replicate.

Two types of photoelastic coatings were used (PS-1E and PS-2C supplied by Photolastic Inc., Malvern, PA). Each coating was applied to the samples after the flaw was implanted. The less sensitive coating, PS-1E with a material fringe value of 7.6 ksi/fr/in (131 MPA/fr/in), contained a flaw with the same geometry as the underlying composite laminate. That is, a jeweler's saw was used to cut a flaw in the coating using the flaw in the sample as a template. The more sensitive coating, PS-2C with a material fringe value of 1.9 ksi/fr/in (33.3 MPA/fr/cm), was applied continuously over the cutout or flaw in the sample, i.e., this coating contained no flaw. Modeling clay was used to fill the flaws such that the coating adhesive would not penetrate or fill the flaws in the samples. The coatings had negligible reinforcing effects on the specimens.

Photographs were taken of each specimen during testing. In addition, after failure, samples were sectioned and photomicrographs (60 x mag.) were taken.

---

*Tensile properties were determined for all laminates using unnotched 0.5 in (1.27 cm) wide samples. These tests were performed on an Instron testing machine at a head rate of 0.05 in/min. These results are reported separately.[18]

Experimental Results and Discussion

COD Measurements

Crack opening displacement (COD) gages were used to measure the relative motion of the center of the opposite faces of all notches and holes in the direction of the remote tensile load. The load-COD traces obtained for the crack-like slits are shown in Figure 1 for all laminates. Similar traces were obtained for laminates containing square slots and circular holes. In general, as indicated by Figure 1, the $[0°/\pm45°/0°]_{2s}$ samples exhibited nearly linear response while that of the $[0°]_{8s}$ and $[\pm45°]_{4s}$ were highly non-linear. Displacements exceeded the range of the COD gage for the latter two orientations.

Gagger and Broutman[8] attributed non-linear behavior and discontinuities in COD measurements to deformations at the notch tips. They suggested a compliance matching procedure to quantify the amount of actual or apparent crack extension at any arbitrary load level.

In the following, for comparison purposes, we will assume that the compliance procedures suggested by Gagger and Broutman can be used for all notches and holes, i.e., crack-like slits, square slots and circular holes. Our calculations are based upon the assumption of self-similar crack growth. It is recognized, however, that actual self-similar growth of the implanted flaw may not have occurred and that the change in compliance may represent local damage or microcracking.

As illustrated in Figure 1, the initial compliance was taken as the inverse of the initial gradient or slope of the straight portion of the load-COD response. The final compliance was taken as the inverse of the slope of the line drawn from the origin to the point of final

fracture on the load-COD response. These values were multiplied by the specimen thickness, t, to eliminate variations caused by this parameter.

The results of the above calculations for initial and final compliances are shown in Figures 2-4. Final compliances are not shown for the $[0°]_{8s}$ and $[\pm45°]_{4s}$ laminates as the extensions exceeded the range of the COD gage. In addition, due to their non-linear nature, it was unclear whether final compliances would have been very meaningful anyway.

In general, the square slots and circular holes were more flexible than the slits for the same aspect ratios as is evident by the respective higher values of compliances shown in Figures 2-4. Presumably, the removal of the extra material in the case of slots and holes lowered the restraint against deformation in those cases. That is, while damage zones might have had comparable linear dimensions transverse to the load, dimensions in the direction of the load were likely larger for the cases of slots and holes as opposed to the case of narrow slits. In other words, the areas of damage were likely greater for slots and holes than for slits of the same aspect ratio.

Using the initial and final compliance curve for a laminate, the amount of real crack extension or damage zone size growth prior to catastrophic fracture was obtained. Consider for example the $[0°/\pm45°/0°]_{2s}$ laminate with a narrow slit of initial aspect ratio of $2a/w = 0.25$. As shown in Figure 2, the total amount of crack extension, including both tips, was found by measuring the horizontal relative distance between the final and initial compliance curves where the value $2a/w = 0.25$ was located on the final compliance curve. Use of the same

procedure for square slots as for narrow slits indicated little self-similar type growth for slots in $[0°/\pm45°/0°]_{2s}$ laminates. On the other hand, self similar growth appeared about equal for slots and slits in the $[0°/90°]_{4s}$ laminate. Such arguments tend to indicate large differences between the fracture behavior of square slots and narrow slits in $[0°/\pm45°/0°]_{2s}$ materials and close similarities in the fracture behavior of square slots and narrow slits in $[0°/90°]_{4s}$ laminates.

Critical Fracture Stresses

Figure 5 shows the average values of the critical gross stresses for the various types of geometries and aspect ratios. The square slots always fractured at a higher stress level than narrow slits irrespective of the aspect ratio or laminate orientation. Thus, stresses would be expected to be somewhat lower at the flaw tip in slots as opposed to slits.

The $[\pm45°]_{4s}$ laminates with holes fractured at about the same or slightly smaller stresses than the same laminates with narrow slits of the same aspect ratios. Examination of the photoelastic fringes in the birefringence coatings shown in Figure 6a and 6c tends to indicate that the dimensions of the region of intense stress gradient or intense energy were larger for the hole than for the crack at about the same remote stress level. Thus fracture stresses of smaller magnitude for the holes were considered reasonable. This information coupled with that of Figure 4 tended to indicate that the holes were more critical than cracks for our $[\pm45°]_{4s}$ laminates.

The trends of variation of the remote critical stress with aspect ratio were the same for all cutouts for all laminates. This observation tends to substantiate the so-called "Materials Science Model"[20,] for fracture by which notch or flaw geometry does not have a major influence on laminate strength and where strength is more closely related to the size and shape of the damage zone surrounding the flaw tip.

It was interesting to note the difference in the character of the variations of critical stress with aspect ratios as shown in Figure 5. The variations for $[0°/\pm45°/0°]_{2s}$ and $[0°/90°]_{4s}$ laminates were similar to that normally encountered in metals and other isotropic materials. In contrast, the variations for the $[0°]_{8s}$ and $[\pm45°]_{4s}$ were of a decidedly different character. It was felt that these differences might be partially attributable to a difference in the mode of crack or damage zone size growth. For the $[0°/\pm45°/0°]_{2s}$ and $[0°/90°]_{4s}$ laminates substantial self similar growth was noted. Axial splitting was the primary crack growth mode for the $[0°]_{8s}$ laminates and crack growth at 45° to the load was the primary fracture mode for the $[\pm45°]_{4s}$ laminates.

Birefringent Coatings

Figures 6-9 represent typical results obtained for each laminate type using both continuous and perforated coatings. The birefringence observed (see Figures 6a and 6c, 7a and 7c, and 8a and 8d) indicated that the intense stress or energy region adjacent to cracks, circular holes and square holes were similar with one another for comparable loads and laminate orientations. Again, this observation tends to substantiate the "Materials Science Model" for fracture[20,21].

The major difference between the isochromatics observed with continuous as opposed to perforated coatings was that the former, even though a more sensitive coating was employed, exhibited less dense fringe patterns than the latter. (Note Figures 6c and 6e.) Also, examination of all Figures 6-9 shows that for continuous coatings, stress concentration sites at opposite edges of holes and cracks tended to interfere with each other.

In general, for $[\pm 45°]_{4s}$ laminates, the fringe pattern was more dense in the +45° direction than the -45° direction adjacent to the hole. As the outer ply was in the +45° in each case, this observation merely indicated that the outer ply was constrained by the inner ply to give this effect.

As illustrated by Figures 7 and 8, the intense stress region for both $[0°]_{8s}$ and $[0°/90°]_{4s}$ laminates was in the direction of the load and/or the 0° fibers. In the former the isochromatics extended completely to the grips prior to failure while in the latter case they did not. This was taken as evidence of axial splitting in both cases. Apparently, the 90° plies in the $[0°/90°]_{4s}$ laminates prevented complete axial splitting of the 0° layers prior to final fracture.

The isochromatic patterns for the $[0°/\pm 45°/0°]_{2s}$ laminates were generally similar to those in isotropic materials, i.e., note the butterfly wing shaped pattern in Figure 9d-9f. The direction of initial notch tip fracture tended to correspond to the angle of inclination of the fringes at the notch tip.

No effort was made to quantify the birefringence results. As pointed out by Dally and Alfirevich,[22] the mismatch between the

properties of the coating and the underlying material (Poisson's ratios and moduli) as well as the anisotropy of the laminate creates difficulties for proper fringe interpretation. Further, our properties were not constant and changed with stress level similar to the results reported by others.[23] Perhaps more importantly, fringe interpretation was made difficult because of uncertainties relative to the nature and strength of the singular stress field for the narrow slits or cracks and square slots. That is, the nature of the singularity of the laminate was likely quite different than the nature of the singularity in either the perforated or the continuous coating.

In-situ and Post Failure Examinations

Each replicate with a coating was examined visually for evidence of stable crack growth during the test. Observations of the birefringence were made as described in the previous section and also the opposite sides of the laminates were inspected as well. On one replicate a microscope was used to examine likely fracture or crack growth sites. Specimens were examined after failure and some samples were sectioned and photomicrographs were taken.

As may be noted by further inspection of Figures 6-9, final fracture planes were generally in the direction of the fibers for $[\pm 45°]_{4s}$ and $[0°]_{8s}$ laminates but were generally self-similar for $[0°/90°]_{4s}$ laminates. The final fracture planes for the $[0°/\pm 45°/0°]_{2s}$ laminates were quite jagged with some 0° and 45° plies separating generally along 45° directions while other 0° and 45° plies separated normal to the load. No distinction in crack growth behavior with aspect ratio was noted for

notch tips or laminate orientations.

Figure 10 is a schematic representation of the stable crack growth observed through the microscope. Such observations were difficult to make as it was not possible to look at all stress concentration sites (front and back and each corner) simultaneously. However, the following remarks regarding observations of stable crack or damage zone growth are thought to be generally proper for the cases investigated.

As mentioned earlier and as noted in Figure 10a, axial splitting was the initial fracture mode for the $[0°]_{8s}$ laminates. It was possible to observe this type of crack growth for such laminates and to note that axial growth continued to the grips long before final separation. Final fracture was always quite explosive with fragments being expelled considerable distances from the test machine. After fracture, nearly total separation of fibers and matrix was obvious. That is, final fracture involved extensive fiber breakage, fiber-matrix debonding, etc. Audible noise was heard throughout each test, often accompanied by axial crack growth and small load perturbations or reductions.

Figure 10b indicates the types of initial crack growth noted for the $[0°/90°]_{4s}$ laminates. Initial growth was usually axial splitting. However, as noted schematically in Figure 10b, for one specimen containing a narrow slit, ($2a/w = 0.35$), the initial growth was self similar for a short distance ($\sim$ 1-2 mm). Axial splitting ($\sim$ 4 mm) then proceeded from the tip of the self similar growth. Final fracture was always self similar (see Figure 8). Again, audible noise was heard throughout each test often with the stable growth described above and small load perturbations or reductions. Significant load reductions were noted at

$\sim$ 80-90% of ultimate load.

For one $[0°/\pm45°/0°]_{2s}$ laminate containing a narrow slit (2a/w = 0.25), self similar growth was noted for $\sim$ 1/2 mm followed by growth at 45° as noted in Figure 10c. In all other cases only stable initial growth at 45° was noted. For the narrow slits, audible noise and load reductions at 80-90% of ultimate accompanied the stable growth. No stable growth or load reductions were observed for square holes. Little noise was heard.

For all $[\pm45°]_{4s}$ laminates, initial stable growth was observed in the outer ply as noted in Figure 10d and exhibited in Figure 11. Interestingly, when the test machine was stopped (fixed grip condition) to observe and photograph the amount of growth, the cracks continued to grow. This may be viewed in Figure 11 together with an apparent necking phenomenon. Because of the obvious time dependent nature of the process, it was decided to see if a delayed fracture process could be observed. The results are amply demonstrated in Figure 12 which represents the variation of remote tensile stress with time for several samples containing cricular holes. For two samples (2a/w = 0.35 and 0.45), the process was allowed to continue until final rupture occurred. For these tests, even though remote stresses were relaxing or decreasing with time, creep or stable crack growth was observed in the outer plies. In other words, relaxation of both the outer ply and remote stresses occurred as the crack grew in the outer ply. Some stress was transmitted to the inner plies causing additional crack growth in the interior. In this way over-all specimen relaxation was possible with creep rupture of individual plies. For these cases stresses were within a few percent

of the ultimate load.

Post failure microscopic examination of all notched and unnotched samples revealed the existence of a large number of microcracks in all free edges. Typical cracks are shown in the micrographs presented in Figure 13 for several laminates containing narrow slits. A schematic in the same figure illustrates the location of the photomicrographs, i.e., on the free edge of machined crack and on the specimen free edge. As may be observed, numerous cracks were found between plies and even within plies. Microscopic examination of numerous specimens clearly indicated more pronounced microcracking effects on the crack free surface as opposed to the specimen free surface.

For our $[0°/\pm45°/0°]_{2s}$ laminates, cracks were always present between the ±45° interface at the specimen free edge. At times such cracks would branch and connect to cracks between either the 0°/-45° or 0°/+45° interfaces respectively. Cracks were als alwavs present between the two 90° middle plies of the $[0°/90°]_{4s}$ laminates at the specimen free edge (see Figure 13). Often, this crack would extend all the way to the gripped regions. The most extensive cracking of all laminates was noted for the $[\pm45°]_{4s}$ samples in which microcracks or delaminations were present between all plies. Such cracks were more pronounced at the specimen free edges for notched laminates than for unnotched laminates. This, perhaps, indicated that the notches adversely affected the stress state at the specimen free edge.

Fracture Mechanics Analysis

As mentioned in the introduction, many efforts have been made to use LEFM for composite materials. In order to force agreement between

analysis and theory, some techniques assume a damage zone at the flaw tip. That is, the crack length is increased by adding an amount which is characteristic of a particular laminate. In the following, comparisons of the characteristic length needed for the point and average stress criteria of Whitney et al.[5] and the inherent flaw model of Waddoups, et al.[1] are presented and compared to the COD method of Gagger and Broutman. Further, fracture toughness as given by the two former methods are compared to those obtained on the basis of the boundary integral equation (BIE) method of Cruse.[24]

Characteristic Lengths

The point and average stress criteria of Whitney et al. and the inherent flaw model of Waddoups et al. can be expressed as, respectively,[5,1]

$$\frac{\sigma_n^{\infty}}{\sigma_u} = \begin{cases} (1 - \xi)^{1/2} \\ [(1 - \xi)/(1 + \xi)]^{1/2} \\ [a_o/a + a_o]^{1/2} \end{cases} \qquad (1)$$

where σ_n^{∞} is the ultimate tensile strength of an infinitely wide plate with a center crack, σ_u is the unnotched laminate strength, $\xi = \frac{a_o}{a + a_o}$ and a is the half crack length. The parameter a_o is defined as the characteristic length for each model. Further, $\sigma_n^{\infty} = Y\sigma_n$ where Y is a finite width correction factor and σ_u is the ultimate unnotched strength of the finite width test specimen.

As all the values necessary were available from our test data for narrow slits, equations (1) were used to calculate the characteristic lengths for the laminates tested for all aspect ratios. The results are

shown plotted in Figures 14 and 15. In addition, the characteristic length as determined from COD measurements using the compliance method explained earlier are given in Figure 15.

For a given laminate all trends are similar regardless of the criterion used. However, the trends for the $[0°]_{8s}$ and $[45°]_{4s}$ laminates are opposite to those of the $[0°/90°]_{4s}$ and $[0°/\pm45°/0°]_{2s}$ laminates. These differences may be due to non-self-similar crack growth in the former two cases contrasted with the quasi-self-similar growth in the last two cases. It should be noted that the average stress criterion gave characteristic lengths so large that the equivalent crack lengths, $2(a + a_0)$, were larger than the width of the specimen for the $[\pm45°]_{4s}$ laminates. This fact may be related to the viscoelastic or delayed failure nature of these laminates or non-self-similar growth discussed earlier. In any event, use of the theories cited for $[\pm45°]_{4s}$ laminates would have to be viewed with skepticism.

Our results, as displayed in Figures 14 and 15, indicated that characteristic lengths as determined by the average stress criterion were about twice those of the inherent flaw model. This confirms Tsai's observation that these two theories are operationally the same except for a factor of two in the definition of the characteristic length.[25]

Characteristic lengths as determined by the COD method were consistent with those of the inherent flaw model for the $[0°/\pm45°/0°]_{2s}$ laminate. For the $[0°/90°]_{4s}$ laminate trends were opposite to those of the other three theories.

Using the characteristic lengths determined by the three theories mentioned above, the fracture toughness, K_Q, of the specimens containing

narrow slits were calculated with the aid of equations given for this purpose by the same three theories. Table 1 represents a comparison of these fracture toughnesses. Also shown in Table 1 are the values calculated using a numerical boundary integral equation (BIE) method based upon anisotropic fracture mechanics. This latter method requires no knowledge of characteristic lengths for K_Q calculations.

Toughnesses calculated by the point and average stress criteria were in close agreement with each other. The BIE method, though slightly lower, is in good agreement to the point and average stress values. The inherent flaw model gave consistently high fracture toughnesses. The fracture toughnesses tended to converge to a common value for all aspect ratios greater than 0.25 for all laminates except $[0°]_{8s}$. In the latter case, nonconvergence likely was the result of non-self-similar crack growth.

Listed in Table 2 are the K-calibration factors for isotropic finite width plates and those necessary for the finite width anisotropic laminates tested. As may be noted, isotropic and anisotropic values are reasonably similar with differences between the two generally being less than 10%.

Summary and Conclusions

The results presented herein have indicated that critical fracture stresses for $[0°]_{8s}$, $[0°/90°]_{4s}$ and $[0°/\pm45°/0°]_{2s}$ laminates containing square holes were only slightly higher than those containing narrow slits or cracks. Circular holes for $[\pm45°]_{4s}$ laminates were slightly more critical than narrow slits. On the other hand, COD measurements

indicated much higher specimen flexibilities for square or circular holes as opposed to narrow slits. Thus, it would seem that from a stress standpoint our results tend to indicate little effect of notch geometry while from a deformation standpoint significant geometry effects were present. In all cases large variations of both critical fracture stresses and COD's were noted for increased aspect ratios.

Birefringence studies indicated similar shaped intense energy or stress regions for all notch geometries and all aspect ratios. Isochromatics were more dense for narrow slits than for holes as expected. Rather than specifically showing damage zone growth, birefringence coatings simply seemed to give results relevant to regions of high stress gradient. This was in contrast to the work of Daniel[12,13]. Differences between our results and his might be due to the kinds of composites investigated and the thickness (number of plies) of the laminates. Our patterns were similar to those obtained by Durchlaub and Freeman.[26]

Birefringence coatings gave good qualitative information relative to regions of high stress. No effort was made to obtain quantitative results from the coatings. Difficulties relative to property mismatches and different singular stress fields in coatings and samples seemed to preclude meaningful quantitative results. Perforated coatinys were obviously better suited for qualitative studies than continuous coatings.

The magnitude of the characteristic length or the size of the damage zone was quite dependent upon the theory used for calculation. This fact seems to emphasize the empirical or two parameter nature of the mathematical models investigated. It should be noted that

characteristic lengths varied substantially with aspect ratio in all cases for all theories. However, variations were most severe for the $[0°]_{8s}$ and $[\pm 45°]_{4s}$ laminates--perhaps indicating the lack of self-similar growth in these cases. The point stress criterion characteristic length varied the least with aspect ratio for all laminates. While a constant characteristic length would in general be inappropriate, it should be noted that if an average or constant value were used, the various theories could likely be used with reasonable confidence for design purposes for both $[0°/\pm 45°/0°]_{2s}$ or $[0°/90°]_{4s}$ laminates.

Crack growth was decidedly non-self-similar for $[0°]_{8s}$ and $[\pm 45°]_{4s}$ laminates. In each case, initial fracture was primarily in the direction of the fibers. For $[0°]_{8s}$ laminates final fracture included extensive fiber breakage, matrix cracking and fiber matrix debonding. Crack growth, while irregular was quasi-self-similar for $[0°/90°]_{4s}$ and $[0°/\pm 45°/0°]_{2s}$ laminates. Initial growth in the latter two cases, as noted by in-situ microscopic observations, indicated similarities with the "Materials Science" fracture model alluded to earlier.[20,21] No obvious difference in crack or damage zone growth was noted as a function of aspect ratio for any laminate.

Photomicrographs gave evidence of extensive microcracking both on the crack free surface and the specimen free surface or edge. Microcracking seemed to be more severe for the former than for the latter. Both intra- and interlamina cracking was noted.

Fracture toughnesses calculated by the point stress, average stress and BIE methods were in close agreement with each other while those by the inherent flaw model were consistently high. K_Q trends

indicated that larger aspect ratios ($\geq$ 0.25) represented the more reliable fracture tests. K-calibration finite width parameters for the anisotropic laminates tested were only slightly larger ($\leq$ 10%) than their isotropic counterparts.

The boundary integral equation (BIE) method appears to be an excellent numerical fracture mechanics approach to investigate the fracture behavior of composite laminates.

It should be recalled that pronounced viscoelastic effects were observed at high stress level for the $[\pm 45°]_{4s}$ laminates. A delayed or creep to failure phenomenon was observed even though the overall specimen was undergoing stress relaxation.

In conclusion, it should be noted that the fracture of composite laminates is a complex process. Both experimental observations and analytical calculations are often an over-simplification of the total process. However, it is our conclusion that there are at least two distinctly different processes involved in initial and final fracture. Initial fracture seems to inevitably be related to matrix cracking and fiber-matrix debonding in all cases. Final fracture seems to inevitably be related to fiber fracture in most cases, e.g., $[0°]_{8s}$, $[0°/90°]_{4s}$ and $[0°/\pm 45°/0°]_{2s}$. Interply delaminations seem to be intermingled in both processes for all laminates but is a primary final fracture mode for the $[\pm 45°]_{4s}$ laminates.

Acknowledgement

The financial support provided for this work by NASA Grant NSG 2038 from the Materials and Physical Sciences Branch of the NASA-Ames Research Center is gratefully acknowledged. We would especially like to thank D. P. Williams and his colleagues of NASA-Ames for their many helpful suggestions and criticisms. Thanks are especially due to Dr. T. A. Cruse for his generosity in providing the authors with tapes of his BIE analysis for our use free of charge.

References

1. Waddoups, M. E., Eisenmann, J. R., and Kaminski, B. E., "Macroscopic Fracture Mechanics of Advanced Composite Materials", Journal of Composite Materials, Vol. 5, 1971.

2. Sih, G. C., and Liebowitz, H., "Mathematical Theories of Brittle Fracture", Fracture, Academic Press, New York, 1968.

3. Cruse, T. A., and Osias, J. R., "Exploratory Development on Fracture Mechanics of Composite Materials", Technical Report AFML-TR-74-111, April 1974.

4. Konish, H. J., and Cruse, T. A., "Determination in Orthotropic Graphite-Epoxy Laminates", Composite Reliability, ASTM STP 580, 1975.

5. Nuismer, R. J., and Whitney, J. M., "Uniaxial Failure of Composite Laminates Containing Stress Concentrations", Fracture Mechanics of Composites, ASTM STP 593, 1975.

6. Morris, D. H., and Hahn, H. T., "Fracture Resistance Characterization of Graphite/Epoxy Composites", Composite Materials: Testing and Design, ASTM STP 617, 1977.

7. Phillips, D. C., and Tetelman, A. S., "Fracture Toughness of Fiber Composites", Composites, Vol. 3, 1972.

8. Gagger, S., and Broutman, L. J., "Crack Growth Resistance of Random Fiber Composites", Journal of Composite Materials, Vol. 9, July 1975.

9. Brinson, H. F., and Yeow, Y. T., "An Experimental Study on the Fracture Behavior of Laminated Graphite/Epoxy Composites", Composite Materials: Testing and Design, ASTM STP 617, 1977.

10. Kanninen, M. F., Rybicki, E. F., and Griffith, W. L., "Preliminary Development of a Fundamental Analysis for Crack Growth in a Fiber Reinforced Composite Material", Composite Materials: Testing and Design, ASTM STP 617, 1977.

11. Morris, D. H., and Hahn, H. T., "Mixed-Mode Fracture of Graphite/Epoxy Composites" Fracture Strength", Journal of Composite Materials, (in review).

12. Daniel, I. M., "Biaxial Testing of Graphite/Epoxy Composites Containing Stress Concentrations", Mechanics of Composite Review, AFML-TR, Stratford House, Dayton, Ohio, October 1976.

13. Daniel, I. M., "Photoelastic Study of Crack Propagation in Composite Models", Journal of Composite Materials, Vol. 4, April 1970.

14. Cruse, T. A., and Stout, M. G., Journal of Composite Materials, Vol. 7, April 1973.

15. Mandell, J. F., Wong, S. S., and McGarry, F. J., "Fracture of Graphite Fiber Reinforced Composites", Technical Report, AFML-TR-73-142, 1973.

16. Marcus, L. A., and Stinchcomb, W. W., "Measurement of Fatigue Damage in Composite Materials", 1973 SESA Fall Meeting, Indianapolis, Ind.

17. Chang, F. H., Couchman, J. C., Eisenmann, J. R., and Yee, B. G. W., "Application of a Special X-Ray Technique for Monitoring Damage Zone Growth in Composite Laminates", Composite Relability, ASTM STP 580, 1975.

18. Yeow, Y. T., and Brinson, H. F., "A Comparison of Simple Shear Characterization Methods for Composite Laminates", V.P.I. & S.U. Report, VPI-E-77-7, Feb., 1977.

19. Brinson, H. F., and Yeow, Y. T., "An Investigation of the Failure and Fracture Behavior of Graphite Epoxy Laminates", V.P.I. & S.U. Report, VPI-E-75-23, September 1973.

20. Zweben, C. H., "Fracture Mechanics and Composite Materials: A Critical Analysis", Analysis of the Test Methods for High Modulus Fibers and Composites, ASTM STP 521, 1973.

21. Rosen, B. W., Kulkarni, S. V., and McLaughlin, Jr., P. V., "Failure and Fatigue Mechanisms in Composite Materials". Inelastic Behavior of Composite Materials, A.S.M.E., AMD, Vol. 13.

22. Dally, J. W., and Alfirevich, I., "Application of Birefringent Coatings to Glass-fiber-reinforced Plastics", Experimental Mechanics, March 1969.

23. Sendeckyj, G. P., Richardson, M. D., and Pappas, J. E., Composite Reliability, ASTM STP 580, 1975.

24. Snyder, M. D., and Cruse, T. A., "Boundary-Integral Equation Analysis of Cracked Anisotropic Plates", Int. Journal of Fracture, Vol. 11, 1975.

25. Tsai, S. W., and Hahn, H. T., "Failure Analysis of Composite Materials", Inelastic Behavior of Composite Materials, A.S.M.E., AME, Vol. 13, 1975.

26. Durchlaub, E. C., and Freeman, R. B., "Design Data for Composite Structure Safe-life Predictions", AFML-TR-73-225, March 1974.

Table 1. Comparison of Fracture Toughnesses.

Orientation	2a/w	Fracture Toughness, K_Q ksi $\sqrt{in}$ (MPA $\sqrt{cm}$)			
		Point Stress	Average Stress	Inherent Stress	BIE Method
$[0°]_{8s}$	0.15	84.75 (931.41)	84.75 (931.37)	156.28 (1717.33)	84.01 (923.17)
$[0°]_{8s}$	0.25	93.50 (1027.46)	93.50 (1027.46)	134.33 (1476.13)	91.00 (999.98)
$[0°]_{8s}$	0.35	91.86 (1009.43)	91.86 (1009.43)	114.51 (1258.33)	86.94 (955.37)
$[0°]_{8s}$	0.45	77.44 (850.97	77.44 (850.97)	86.4 (949.43)	70.40 (773.61)
$[0°/\pm45°/0°]_{2s}$	0.15	27.67 (304.06)	27.68 (304.17)	33.00 (362.63)	27.70 (304.39)
$[0°/\pm45°/0°]_{2s}$	0.25	31.03 (340.98)	31.02 (340.87)	35.07 (385.38)	30.27 (332.63)
$[0°/\pm45°/0°]_{2s}$	0.35	32.49 (357.03	32.49 (357.03)	35 69 (392.19)	30.79 (338.35)
$[0°/\pm45°/0°]_{2s}$	0.45	32.46 (356.70	32.46 (356.70)	34.77 (382.08)	29.50 (324.17)
$[0°/90°]_{4s}$	0.15	27.99 (307.58)	27.98 (307.47)	32.24 (354.28)	27.50 (302.19)
$[0°/90°]_{4s}$	0.25	31.70 (348.35)	31.71 (348.46)	35.32 (388.13)	30.93 (339.88)
$[0°/90°]_{4s}$	0.35	33.08 (363.51)	33.08 (363.51)	31.90 (349.50)	31.52 (346.37)
$[0°/90°]_{4s}$	0.45	34.67 (380.98)	34.69 (381.20)	36.96 (406.15)	30.59 (336.15)
$[\pm45°]_{4s}$	0.15	10.88 (119.56)	10.88 (119.56)	28.44 (312.52)	10.84 (119.12)
$[\pm45°]_{4s}$	0.25	12.90 (141.76)	12.91 (141.87)	24.09 (264.72)	12.57 (138.13)
$[\pm45°]_{4s}$	0.35	13.73 (150.88)	13.72 (150.77)	21.29 (233.95)	13.14 (144.39)
$[\pm45°]_{4s}$	0.45	14.62 (160.66)	14.62 (160.66)	20.90 (229.67)	13.36 (146.81)

Table 2. K-Calibration Factors for Center Notched T300/934 Graphite-Epoxy Tensile Specimens.

	K-Calibration Factor, F(2a/w)				
2a/w	Isotropic	$[0°]_{8s}$	$[0°/\pm45°/0°]_{2s}$	$[0°/90°]_{4s}$	$[\pm45°]_{4s}$
0.15	1.0095	1.0116	1.0142	1.0108	1.0218
0.25	1.0273	1.0322	1.0406	1.0310	1.0614
0.35	1.0563	1.0688	1.0838	1.0642	1.1237
0.45	1.0993	1.1229	1.1490	1.1469	1.2138

Longitudinal modulus, E_{11} = 19.89 x 10^6 psi (137.14 x 10^3 MPA)

Transverse modulus, E_{22} = 2.17 x 10^6 psi (14.96 x 10^3 MPA)

Shear modulus, G_{12} = 1.22 x 10^6 psi (8.41 x 10^3 MPA)

Poisson's ratio, ν_{12} = 0.352

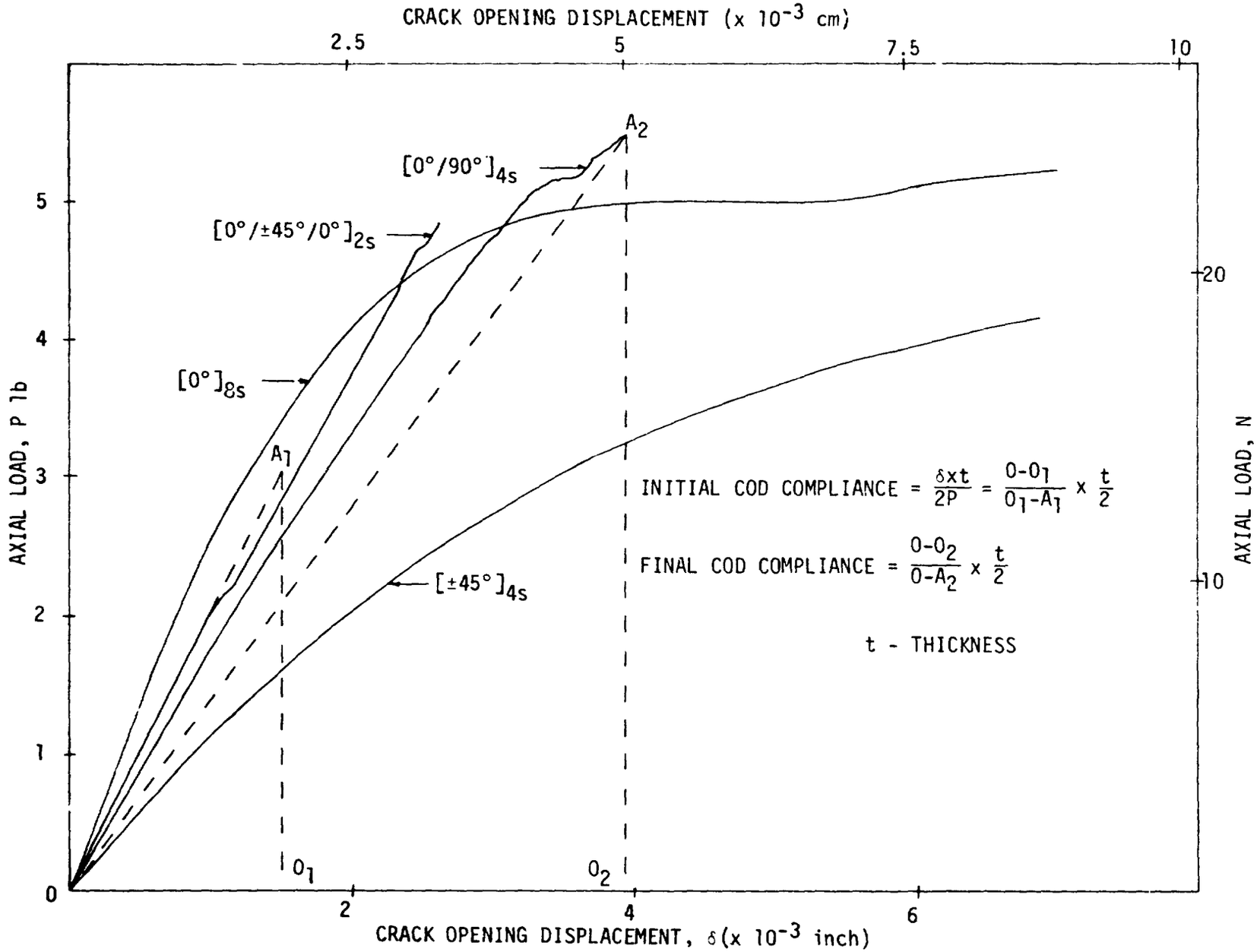

Fig. 1. Load-displacement curves for slits, 2a/w = 0.25.

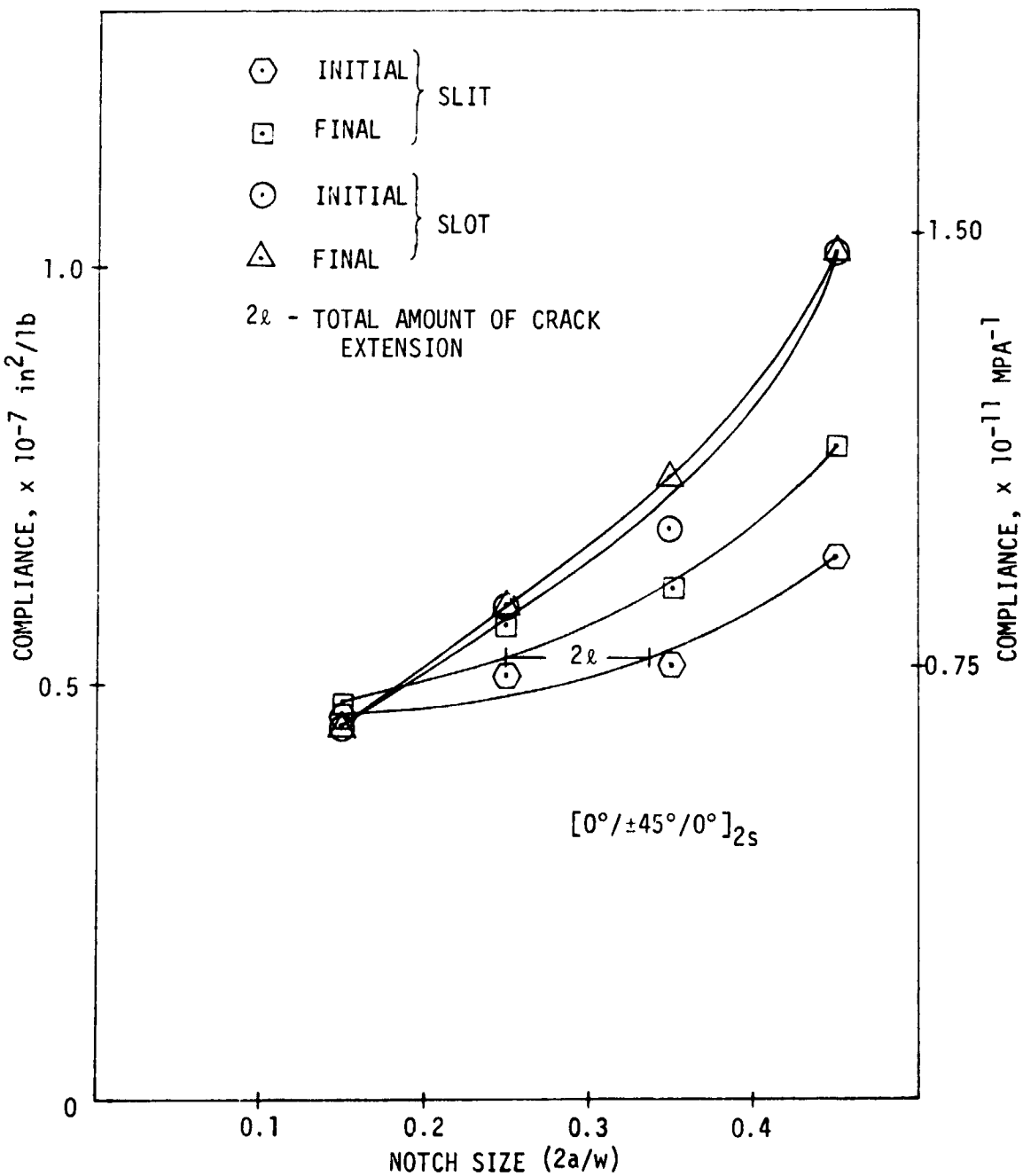

Fig. 2. Compliance vs. Notch Size for $[0°/\pm45°/0°]_{2s}$ Laminate.

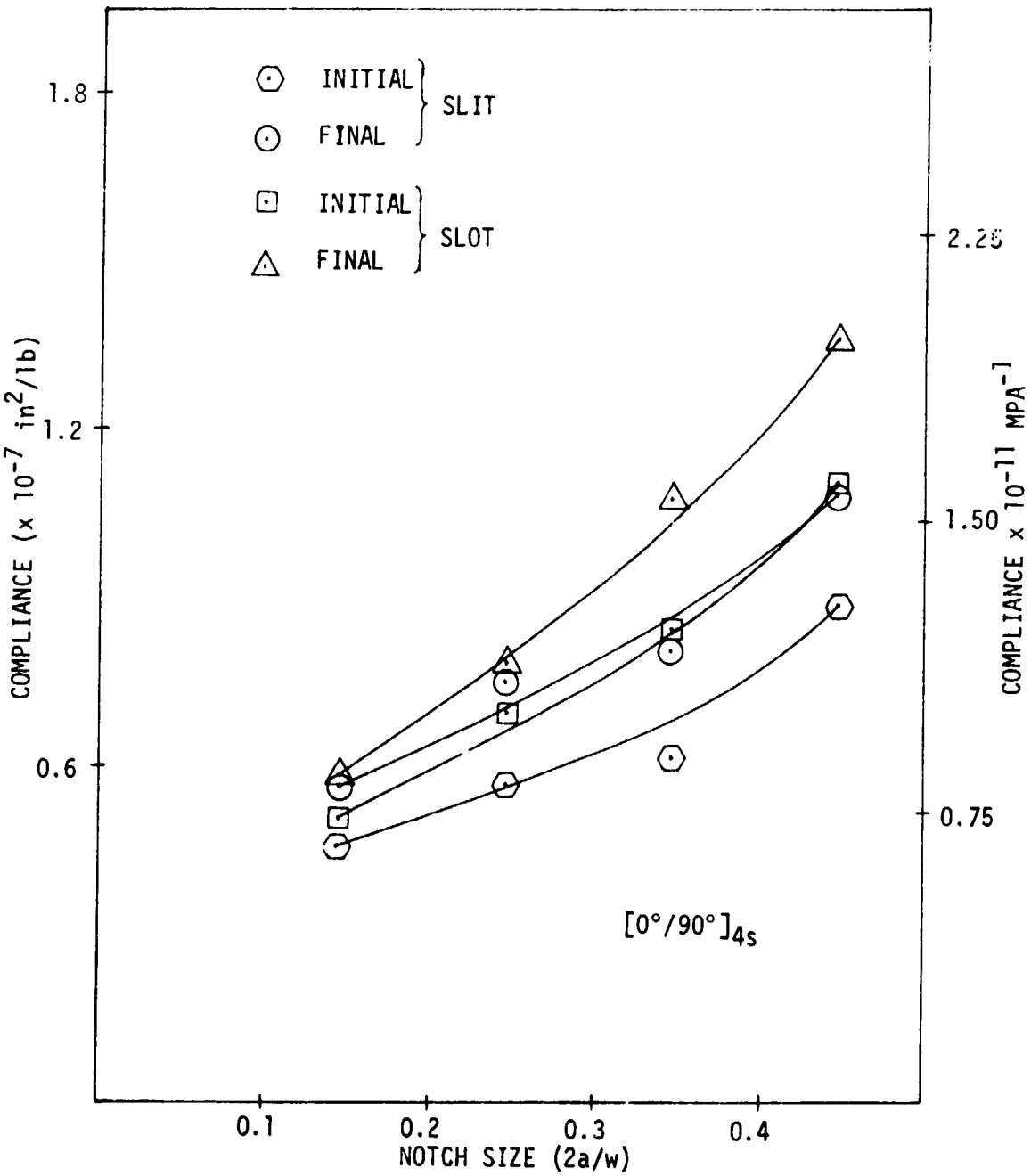

Fig. 3. Compliance vs. Notch Size for $[0°/90°]_{4s}$ Laminate.

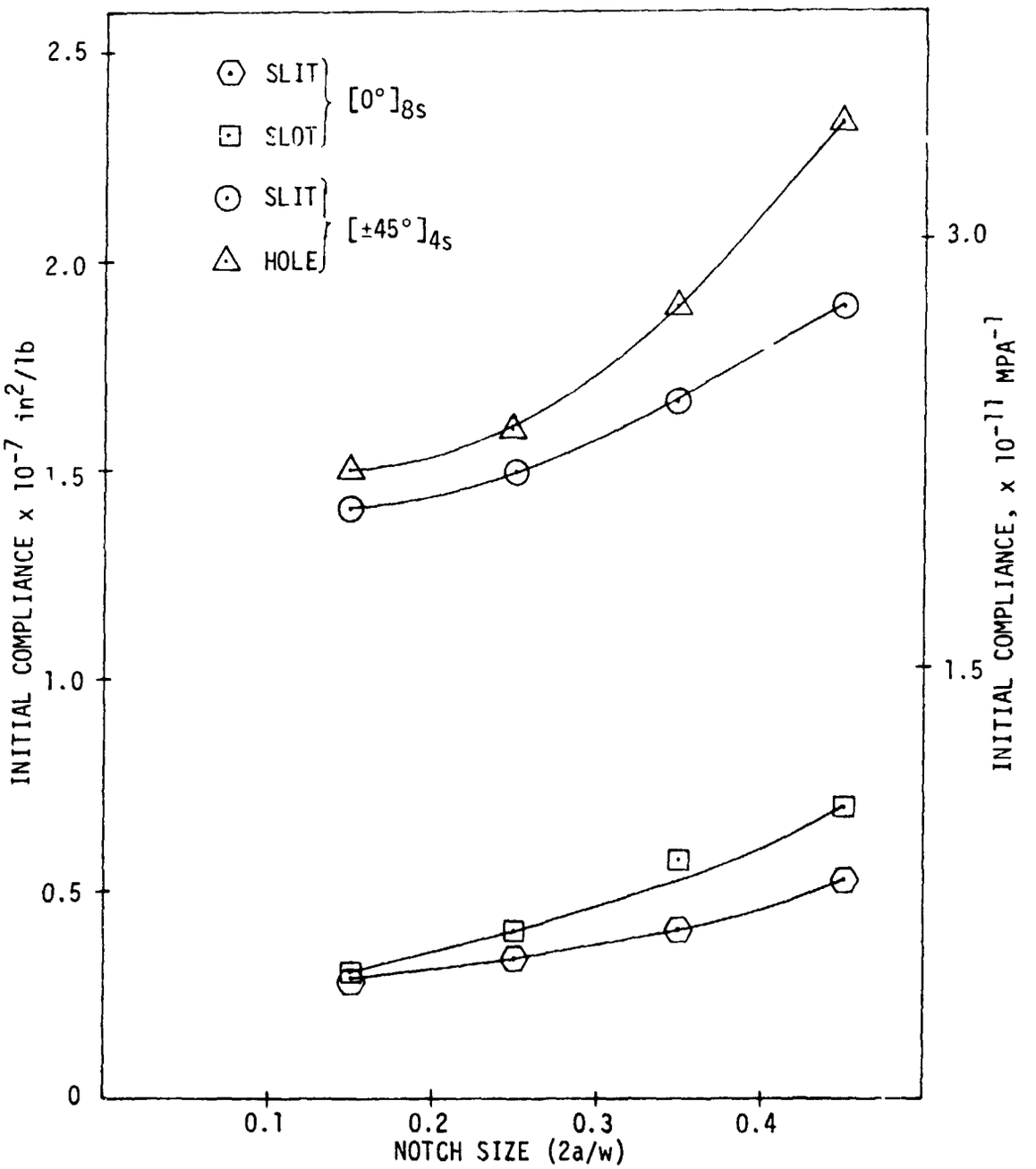

Fig. 4. Compliance vs. Notch Size for $[0°]_{8s}$ and $[\pm 45°]_{4s}$ Laminates.

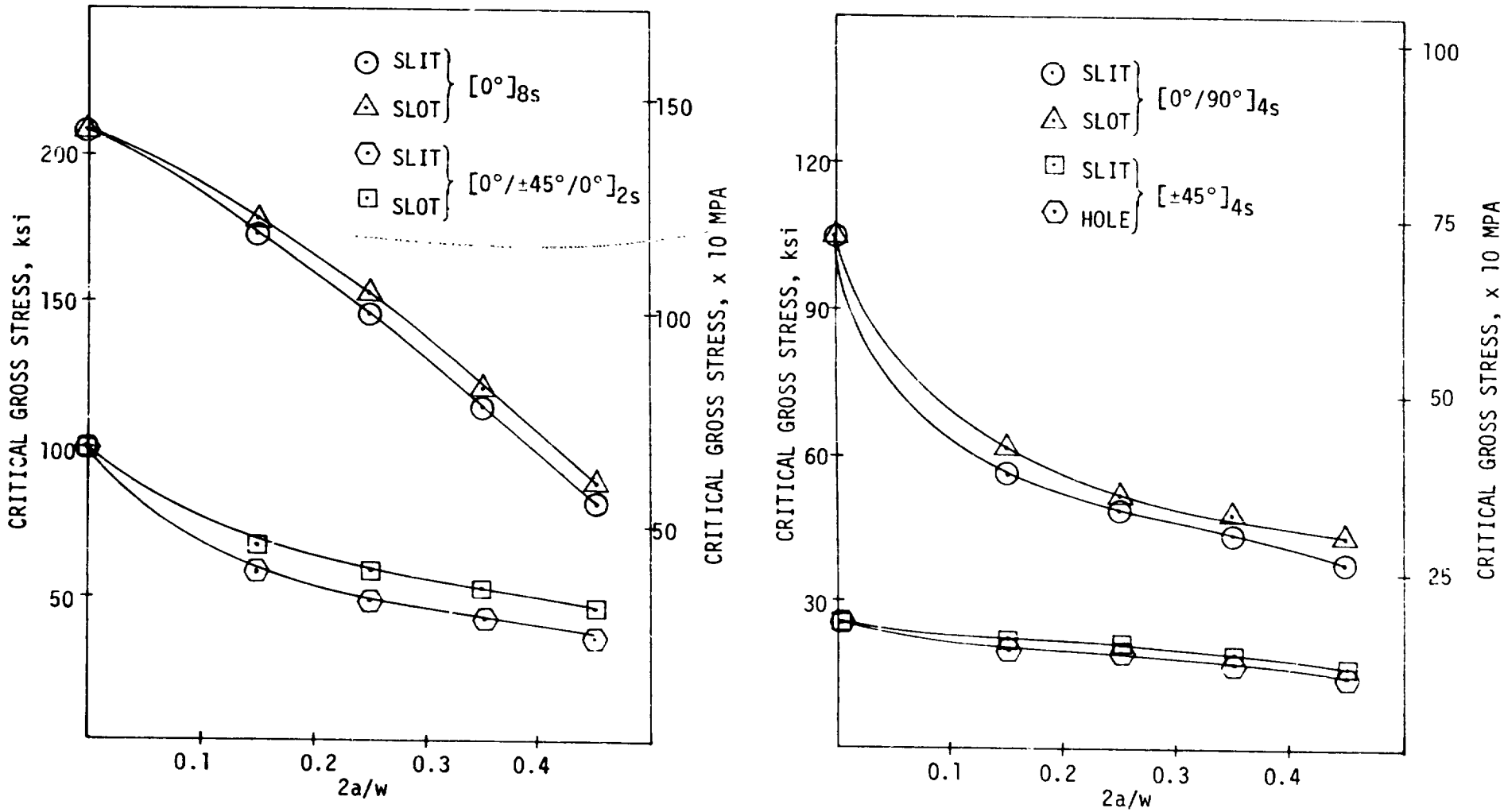

Fig. 5. Remote failure stresses of T300/934 G/E laminates.

a) 13.10 ksi
(90.29 MPA)

b) Fracture

c) 13.22 ksi
(91.16 MPA)

d) Fracture

e) 16.39 ksi
(113.00 MPA)

f) Fracture

Fig. 6. Isochromatics of [±45°] laminate with perforated (a-d) and continuous (e,f) coatings (2a/w = 0.45).

ORIGINAL PAGE IS
OF POOR QUALITY

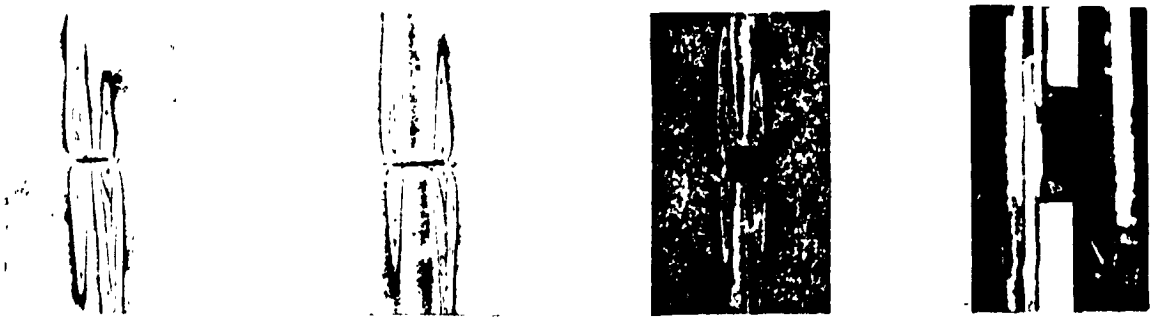

a) 71.78 ksi (494.92 MPA)
b) 53.57 ksi (369.37 MPA)
c) 72.92 ksi (502.78 MPA)
d) Fracture

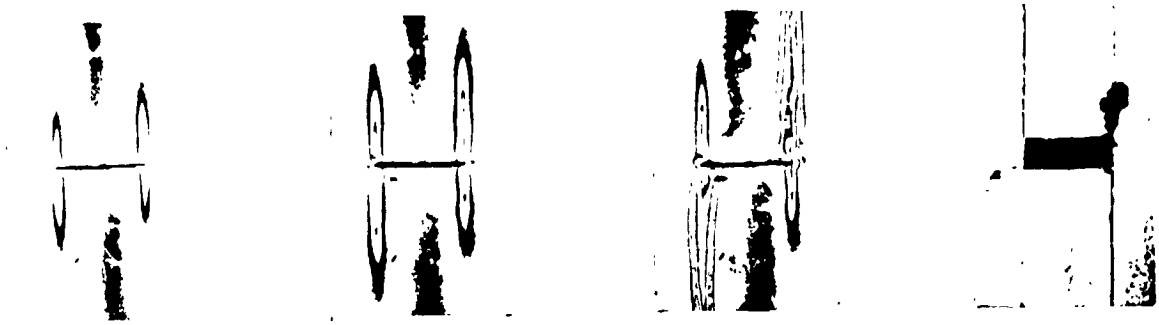

e) 26.61 ksi (183.48 MPA)
f) 33.27 ksi (229.40 MPA)
g) 36.59 ksi (252.29 MPA)
h) Fracture

i) 43.07 ksi (296.97 MPA)
j) 47.72 ksi (329.03 MPA)
k) 53.38 ksi (361.16 MPA)
l) Fracture

a) Slit, 2a/w = 0.15 b) Slit, 2a/w = 0.25 c-d) Slot, 2a/w = 0.15
e-h) Slit, 2a/w = 0.45 i-l) Slot, 2a/w = 0.35

Fig. 7. Isochromatics of $[0°]_{8s}$ laminates with perforated (a-h) and continuous (i-l) coatings.

ORIGINAL PAGE IS
OF POOR QUALITY

a) 46.12 ksi (317.97 MPA)

b) 48.54 ksi (334.71 MPA)

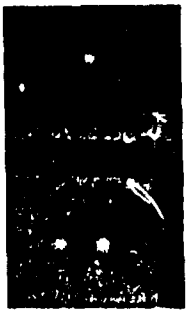

c) Fracture

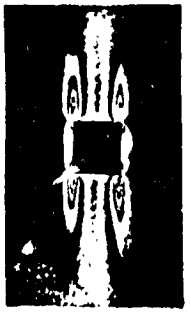

d) 45.81 ksi (315.86 MPA)

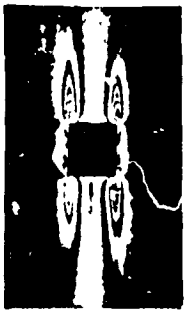

e) 50.15 ksi (345.79 MPA)

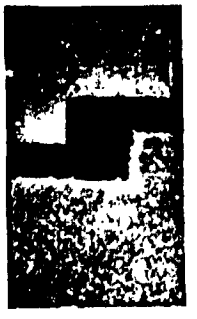

f) Fracture

g) 44.53 ksi (307.06 MPA)

h) 47.32 ksi (326.25 MPA)

i) Fracture

a-c) Slit, 2a/w = 0.25 d-f) Square slot, 2a/w = 0.25
g-i) Square slot, 2a/w = 0.25

Fig. 8. Isochromatics of $[0°/90°]_{4s}$ laminate with perforated (a-f) and continuous (g-i) coatings.

ORIGINAL PAGE IS
OF POOR QUALITY

a) 43.48 ksi (297.78 MPA)

b) 45.45 ksi (313.40 MPA)

c) Fracture

d) 29.21 ksi (201.37 MPA)

e) 39.28 ksi (270.81 MPA)

f) Fracture

Fig. 9. Isochromatics of $[0°/\pm45°/0°]_{2s}$ laminate with continuous (a-c) and perforated (d-f) coatings (slit, 2a/w = 0.25).

ORIGINAL PAGE IS
OF POOR QUALITY

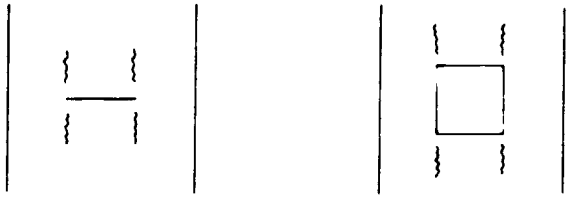

a) $[0°]_{8s}$

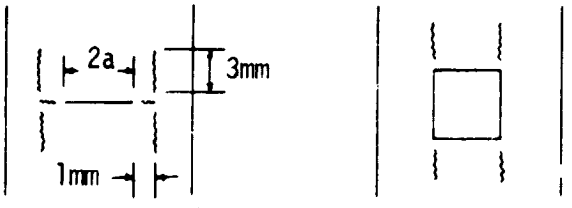

b) $[0°/90°]_{4s}$

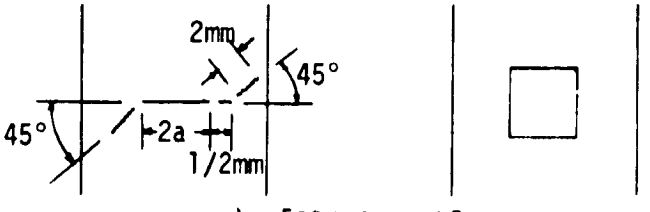

c) $[0°/\pm45°/0°]_{2s}$

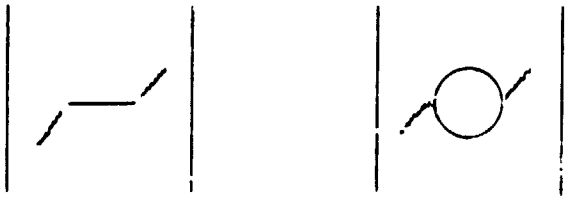

d) $[\pm45°]_{4s}$

Fig. 10. Schematic representation of stable crack growth observations.

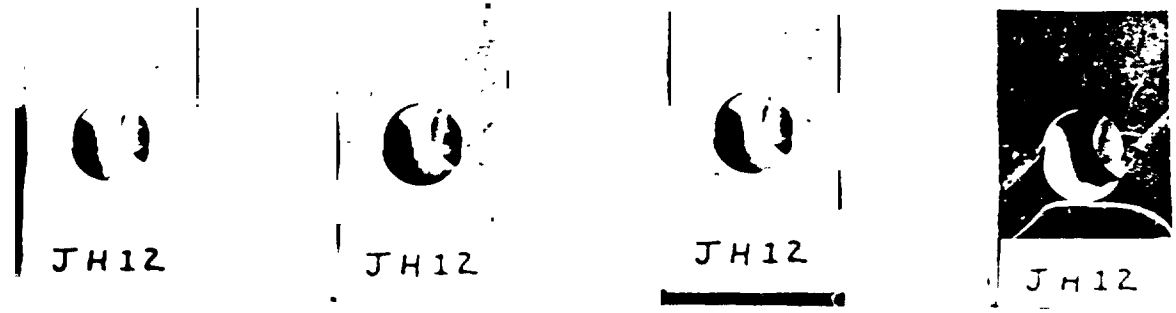

a) 5.47 min. b) 6.14 min. c) 7.00 min. d) 7.22 min.

Fig. 11. Fracture of $[\pm 45^\circ]_{4S}$ laminate with time showing apparent necking.

ORIGINAL PAGE IS
OF POOR QUALITY

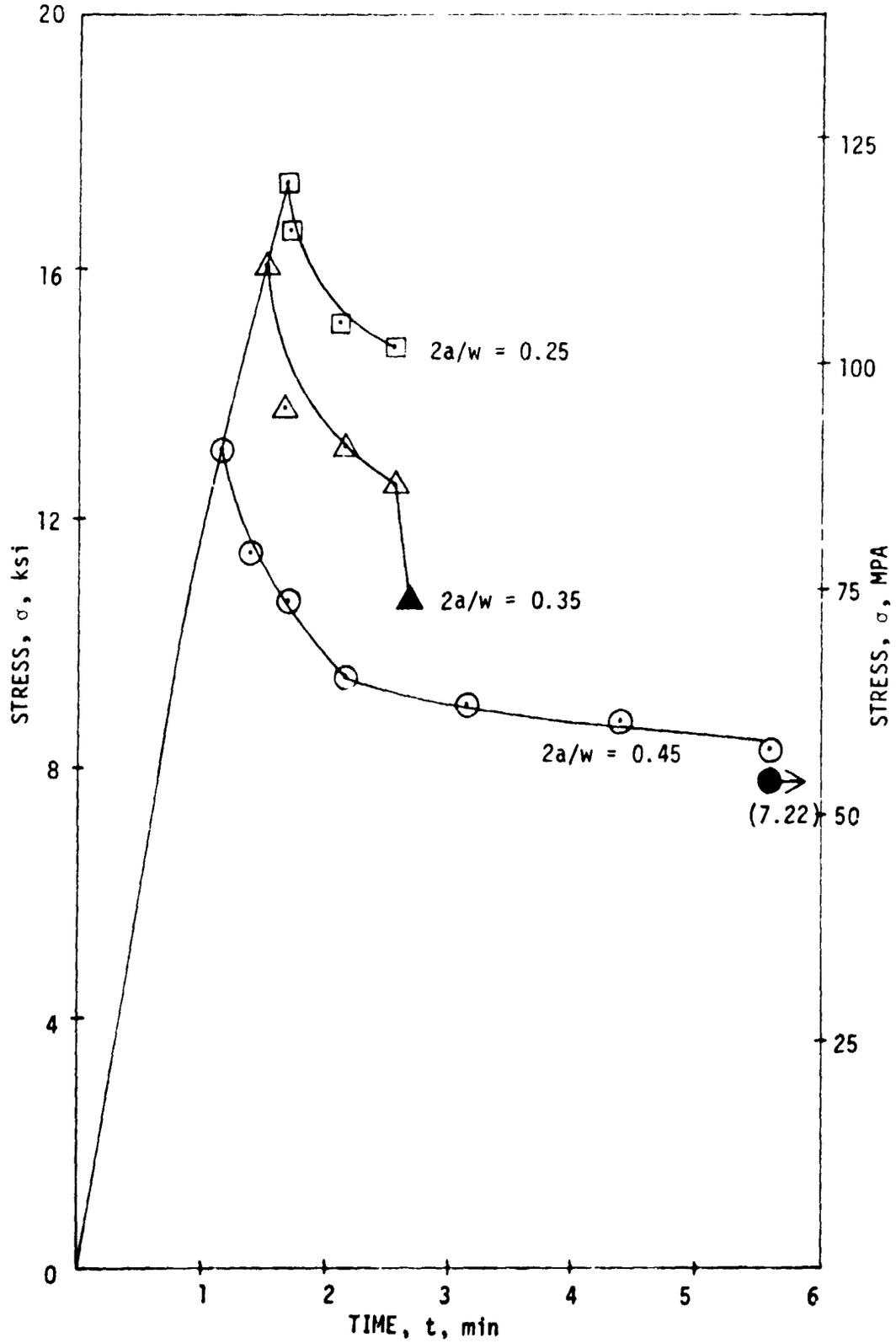

Fig. 12. Delayed or Time Dependent Fracture of $[\pm 45°]_{4s}$ T300/934 G/E with Circular Holes.

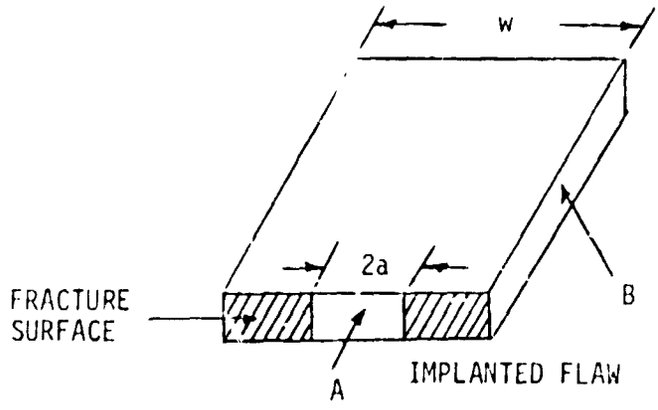

A B

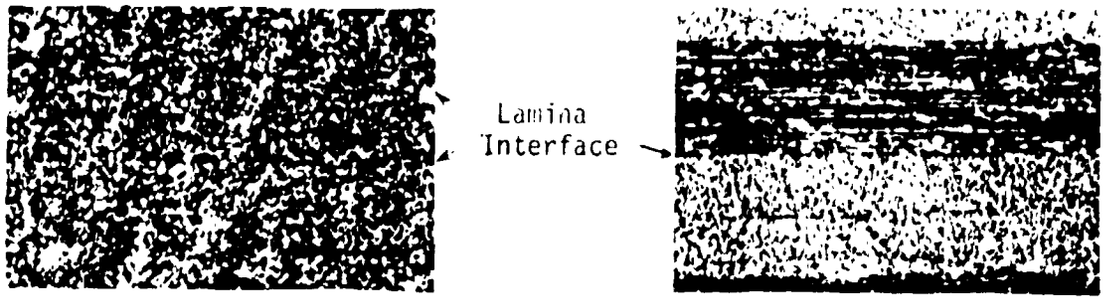

$[0°/\ 45°/0°]_{2s}$

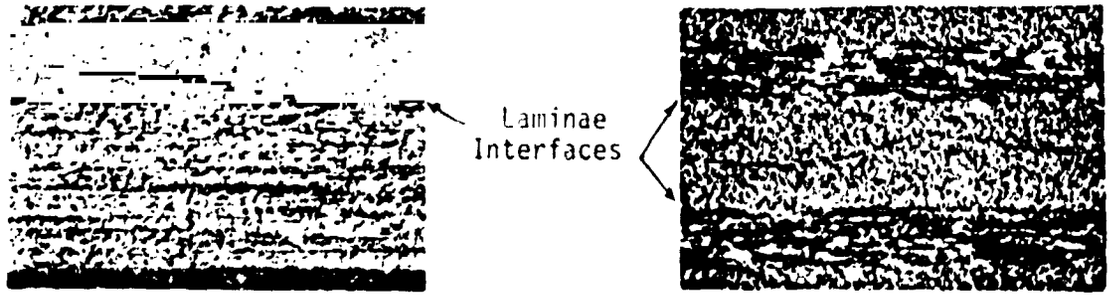

$[0°/90°]_{4s}$

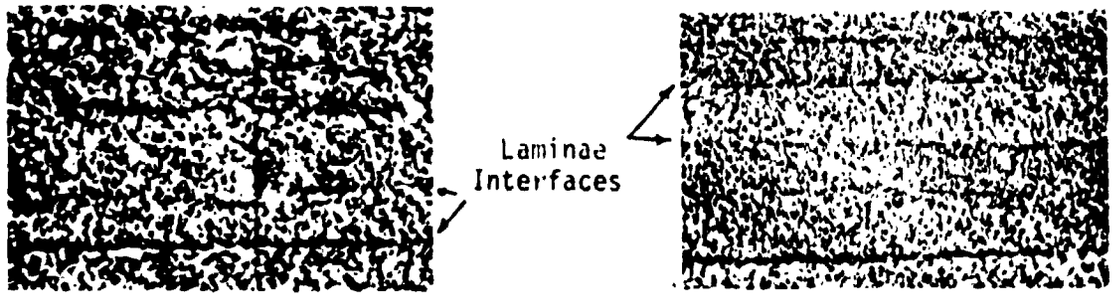

$[\pm 45°]_{4s}$

Fig. 13. Photomicrographs of the free surfaces.

ORIGINAL PAGE IS
OF POOR QUALITY

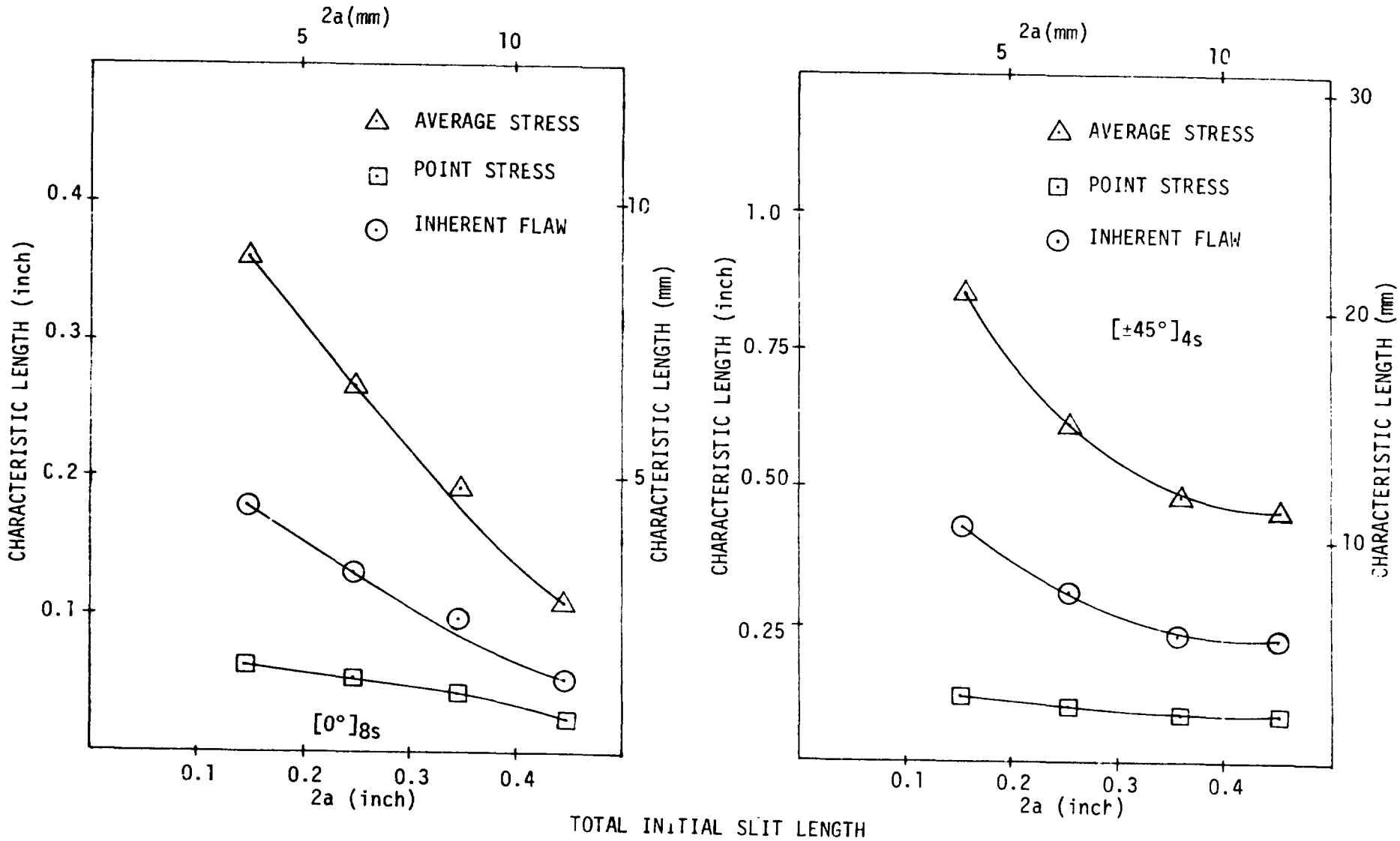

Fig. 14. Characteristic Lengths for T300/934 Laminates with Implanted Cracks.

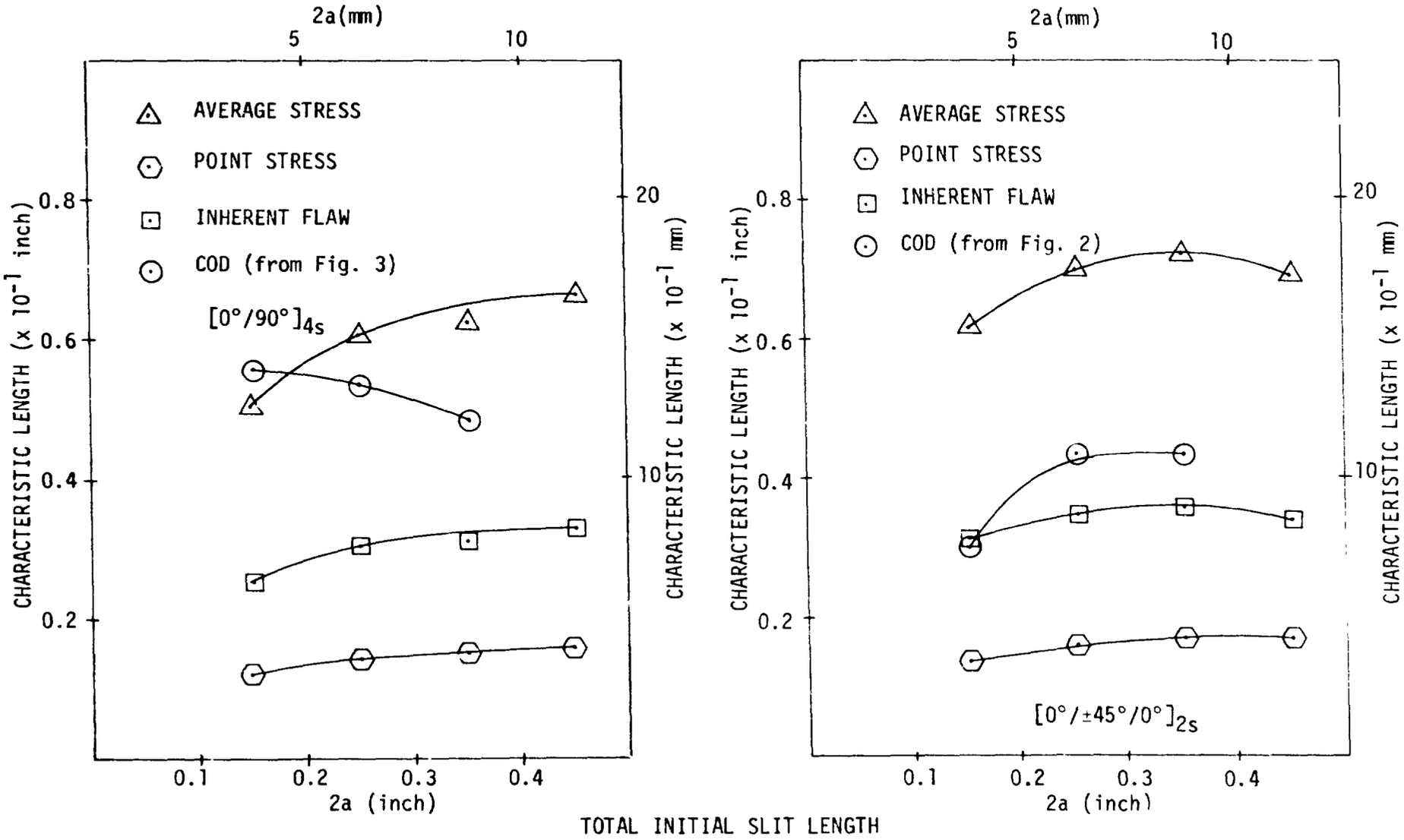

Fig. 15. Characteristic lengths for T300/934 laminates with implanted cracks.

SECURITY CLASSIFICATION OF THIS PAGE (When Data Entered)

REPORT DOCUMENTATION PAGE

READ INSTRUCTIONS BEFORE COMPLETING FORM

1. REPORT NUMBER: VPI-E-77-15	2. GOVT ACCESSION NO.
3. RECIPIENT'S CATALOG NUMBER	
4. TITLE (and Subtitle): A STUDY OF DAMAGE ZONES OR CHARACTERISTIC LENGTHS AS RELATED TO THE FRACTURE BEHAVIOR OF GRAPHITE/EPOXY LAMINATES	5. TYPE OF REPORT & PERIOD COVERED: Interim 10/1/76 - 9/30/77
	6. PERFORMING ORG. REPORT NUMBER
7. AUTHOR(s): Y. T. Yeow, H. F. Brinson	8. CONTRACT OR GRANT NUMBER(s): NASA-NSG 2038
9. PERFORMING ORGANIZATION NAME AND ADDRESS: Engineering Science and Mechanics, Virginia Polytechnic Institute & State University, Blacksburg, VA 24061	10. PROGRAM ELEMENT, PROJECT, TASK AREA & WORK UNIT NUMBERS
11. CONTROLLING OFFICE NAME AND ADDRESS: NASA Materials Science Branch, Ames Research Center, Moffett Field, CA 94035	12. REPORT DATE: May 1977
	13. NUMBER OF PAGES
14. MONITORING AGENCY NAME & ADDRESS (if different from Controlling Office)	15. SECURITY CLASS. (of this report): Unclassified
	15a. DECLASSIFICATION/DOWNGRADING SCHEDULE

16. DISTRIBUTION STATEMENT (of this Report)

Approved for public release; distribution unlimited

17. DISTRIBUTION STATEMENT (of the abstract entered in Block 20, if different from Report)

Approved for public release; distribution unlimited.

18. SUPPLEMENTARY NOTES

19. KEY WORDS (Continue on reverse side if necessary and identify by block number)

Fracture, damage zones, characteristic lengths, graphite/epoxy laminates

20. ABSTRACT (Continue on reverse side if necessary and identify by block number)

The results of uniaxial tensile tests conducted on a variety of graphite/epoxy laminates containing narrow rectangular slits, square or circular holes with various aspect ratios are discussed. The techniques used to study stable crack or damage zone growth--namely, birefringence coatings, COD gages, and microscopic observations are discussed. Initial and final fracture modes are discussed as well as the effect of notch size and shape and laminate type on the fracture process. Characteristic lengths are calculated and compared to each other using the point, average and inherent flaw theories. Fracture toughnesses are

DD FORM 1 JAN 73 1473 EDITION OF 1 NOV 65 IS OBSOLETE

SECURITY CLASSIFICATION OF THIS PAGE (When Data Entered)

Item 20 (continued)

calculated by the same theories and compared to a boundary integral equation technique. Finite width K-calibration factors are also discussed.